X-Band Lightweight Rainfall Radiometer First Light

Christopher Ruf[1] and Caleb Principe[2]

[1]University of Michigan, Ann Arbor, MI 48109 USA
734-764-6561 (V), 734-764-5137 (F), cruf@umich.edu (E)

2. NASA Goddard Space Flight Center, Greenbelt, MD 20771 USA
301-286-8726 (V), 301-286-1750 (F), caleb.principe@gsfc.nasa.gov (E)

***Abstract* - The X-Band Lightweight Rainfall Radiometer (LRR-X) is an aircraft microwave sensor that is under development for the NASA Earth Science Technology Office by Goddard Space Flight Center and the University of Michigan. LRR-X is intended to address several pressing issues related to the Global Precipitation Measurement (GPM) Mission, for which it is a science and technology testbed instrument [1]. LRR-X is a pushbroom imager operating at 10.7 GHz with a $\pm 45^\circ$ cross track field of view and a nominal 1.5° angular resolution at nadir. Simultaneous antenna beams are formed over the entire field of view by synthetic aperture interferometry. LRR-X is scheduled to fly on board the NASA DC-8 research aircraft during May-June 2003. An overview of the instrument's visibility function calibration algorithm is presented, together with a status report on the hardware development.**

I. Introduction

The functional design of the LRR-X prototype aircraft sensor as been described in detail previously [2] Upcoming final integration and test procedures that are scheduled for this year include circle flights at numerous constant bank angles to be flown over the open ocean in clear air and calm sea conditions. This will enable accurate modeling of the expected scenes and will provide a set of end-to-end calibration references. Additional science flights are also scheduled together with other active and passive precipitation sensors. The prototype will provide high fidelity estimates of the image resolution and field of view, absolute calibration, ΔT sensitivity and data rate requirements for the space flight version.

II. Visibility Calibration Algorithm

A schematic block diagram of one of the LRR-X receivers is shown in Figure 1. Only elements necessary to the development of the calibration transfer model are shown. In the figure, T_A represents the input antenna temperature. T_F is the effective physical temperature of the lossy coaxial cable feeding the slotted waveguide antenna to the receiver. L_F is the loss in the feed section. The noise diode power is accounted for by an effective injected noise temperature T_N. The path loss between the noise injection directional coupler and the PIN reference switch is given by L_R at physical temperature T_R. The physical temperature of the reference load at the PIN switch is also assumed to be at temperature T_R. The receiver noise temperature is given by T_{RX}.

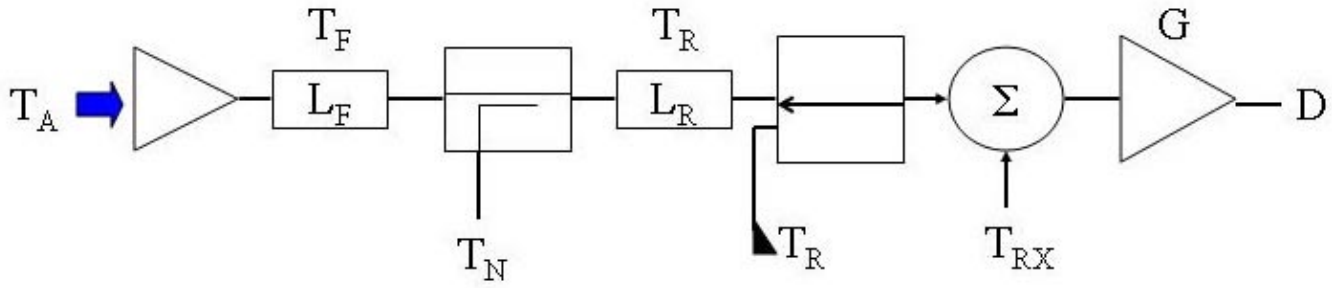

Figure 1. LRR-X receiver schematic block diagram illustrating principle contributors to calibration transfer function.

0-7803-7930-6/$17.00 (C) 2003 IEEE

Self-correlation of antenna samples can be represented as

$$C_{Aii} = [T_{Ai}(1 - L_{Fi})(1 - L_{Ri}) + L_{Fi}T_{Fi}(1 - L_{Ri}) + L_{Ri}T_{Ri} + T_{RXi}]G_{ii} + C_{0ii} \quad (1)$$

where $G_{ii} = G_iG_i$. Self-correlation of noise diode samples can be similarly represented as C_{Nii}

$$C_{Nii} = [T_{Ai}(1 - L_{Fi})(1 - L_{Ri}) + L_{Fi}T_{Fi}(1 - L_{Ri}) + |k_i|^2T_N(1 - L_{Ri}) + L_{Ri}T_{Ri} + T_{RXi}]G_{ii} + C_{0ii} \quad (2)$$

where k_i is the coupling constant associated with the noise diode injection into the signal path of the i^{th} receiver. Note that k_i is, in general, a complex number in order to account for phase differences between the injection of a common noise diode signal into different receivers. Self-correlation of reference load samples can be rewritten as

$$C_{Nii} = (T_{Ri} + T_{RXi})G_{ii} + C_{0ii} \quad (3)$$

Cross-correlation of antenna samples can be written as

$$C_{Aij} = V_{ij}[(1 - L_{Fi})(1 - L_{Fj})(1 - L_{Ri})(1 - L_{Rj})]^{1/2}G_{ij} + C_{0ij} \quad (4)$$

where V_{ij} is the visibility sample corresponding the ij^{th} receiver pair. Cross-correlation of noise diode samples can be written as

$$C_{Nij} = V_{ij}[(1 - L_{Fi})(1 - L_{Fj})(1 - L_{Ri})(1 - L_{Rj})]^{1/2} + |k_i||k_j|e^{j\phi ij}T_N[(1 - L_{Ri})(1 - L_{Ri})]^{1/2}G_{ij} + C_{0ij} \quad (5)$$

where ϕij is the difference in phase between the complex coupling constants k_i and k_j. It could, for example, account for such things as differences in path length of the noise diode distribution lines or differences between the phase transfer functions of the directional couplers in the i^{th} and j^{th} receivers. Cross-correlation of reference load samples can be written as

$$C_{Nij} = C_{0ij} \quad (6)$$

The gain of each receiver considered as a conventional total power radiometer is its self-correlation gain. It is found from the change in self-correlation counts when the noise diode is switched on, or

$$G_{ii}' = (C_{Nii} - C_{Aii})/(|k_i|^2T_N) \quad (7)$$

where $G_{ii}' = (1 - L_{Ri})G_{ii}$. The power transmission coefficient term, $(1 - L_{Ri})$, has been combined with the actual gain term, G_{ii}, because in practice only their product is needed to calibrate the measurements.

The cross-correlation gain between the ij^{th} receiver pair is similarly found from the change in cross-correlation counts when the noise diode is switched on. In this case, however, possible phase rotations of the noise diode signal in the complex plane must be accounted for. The complex difference in counts with the noise diode turned on is given by

$$C_{Nij} - C_{Aij} = |k_i||k_j|e^{j\phi ij}T_N[(1 - L_{Ri})(1 - L_{Rj})]^{1/2}G_{ij} \quad (8)$$

The cross-correlation gain is found by taking the modulus of both sides of (8), or

$$G_{ij}' = |C_{Nij} - C_{Aij}|/(|k_i||k_j|T_N) \quad (9)$$

where $G_{ij}' = [(1 - L_{Ri})(1 - L_{Rj})]^{1/2}G_{ij}$.

Figure 2. LRR-X deployed at NASA Goddard on 24 April 2003. 14 element thinned linear array of X-Band slotted waveguide antennas (copper) are mounted on an extended ground plane (blue) to reduce backlobes.

III. First LRR-X Visibility Measurements

The fully integrated LRR-X instrument was operated outdoors for the first time on 24 April 2003. LRR was located just outside of the west end of Building 5 at Goddard at operated between 15:47 and 16:40 EDT (see Figure 2.). The raw correlation counts were calibrated using the algorithm described in Section II. This calibration algorithm uses a combination of benchtop laboratory characterizations of the subsystems together with simplified theory. There has been no empirical end-to-end system level calibration yet. So these results should be considered very preliminary.

The brightness temperature (T_B) measured by an individual antenna element is shown in figure 3. For a STAR imager, this corresponds to the average value of T_B over the complete $\pm 45^o$ field of view (FOV). The numbers at the bottom of the figure correspond to specific events described below.

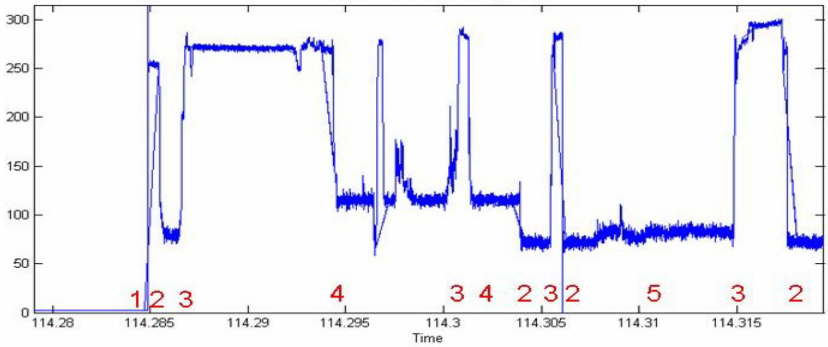

Figure 3. LRR-X FOV-averaged T_B at 10.7 GHz versus elapsed time in fractional days. The numbered events are: 1. Instrument turn on; 2. Observe the zenith sky (zenith is at the center of the $\pm$ 45° FOV so this is average atmospheric downwelling over a wide range of declination angles); 3. Observe a (fairly crude) black body (BB) absorber at ambient temperature; 4. Observe a (fairly crude) step function in T_B by pointing the center of the FOV at the edge of a nearby trailer so that roughly half of the image is clear sky and half is the trailer; 5. Point the center of the FOV at the sun (this was a crude "eyeball" alignment)

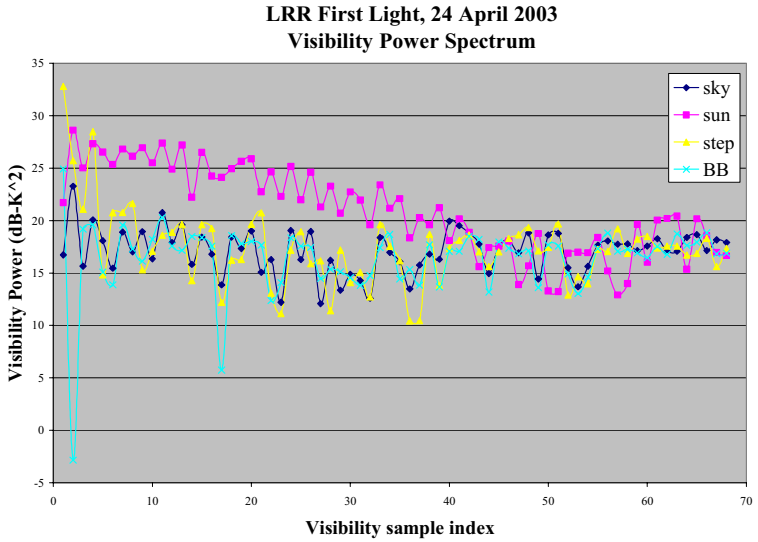

Figure 4. Spatial power spectrum of the TB distribution, as measured by LRR-X for several types of scenes.

The cold sky and hot BB T_Bs in Figure 3 are reasonably consistent with theory and show that the instrument has the proper gain and responsiveness. The intermediate values of T_B for the sun and step function are also reasonable. Resolving the T_B distribution within the FOV requires an inversion of the spatial harmonics measured by the cross-correlation between individual antenna pairs. The spatial power spectrum of the measurements can also be examined for reasonableness. That spectrum is shown in Figure 4 for a few individual samples that were made. The units of "Visibility sample index" on the 'x' axis correspond to the separation between antenna pairs in increments of 0.55λ, where λ is the RF wavelength. Increasing values correspond to higher harmonic components of spatial variability in T_B within the FOV. The BB and sky scenes are the most spatially uniform and their high frequency content is correspondingly lowest and roughly flat. An ideal step function has spatial frequency content which rolls of inversely with frequency. Our step function is far from ideal but it does have a significantly higher power spectrum than that of either the sky or BB at low frequencies but a similar spectrum at higher frequencies. An ideal point source has a broad spatial frequency distribution that does not roll off with frequency. Our sun measurements have significantly higher power at higher frequencies than any of the other cases. All of these results are consistent with theory and indicate that LRR-X is behaving properly.

REFERENCES

[1] Smith, E.A. W.J. Adams, C. Kummerow, C. Principe, C.S. Ruf, T.T. Wilheit "Potential Applications of LRR-STAR Technology for GPM Mission," Proc. of NASA Earth Science Technology Conference, Pasadena, CA, 11-13 June 2002.

[2] Ruf, C., C. Principe, T. Dod, B. Gosselin, B. Monosmith, S. Musko, S. Rogacki, A. Stewart, Z. Zhang, "Lightweight Rainfall Radiometer STAR Aircraft Sensor," Proc. of the 2002 IEEE International Geoscience and Remote Sensing Symposium, Toronto, Canada, II: 850-852, , 2002.